EFDA–JET–PR(07)19

E.A. Lerche, D. Van Eester and JET EFDA contributors

Improved Break-in-Slope Analysis of the Plasma Energy Response in Tokamaks

Improved Break-in-Slope Analysis of the Plasma Energy Response in Tokamaks

E.A. Lerche, D. Van Eester and JET EFDA contributors*

JET-EFDA, Culham Science Centre, OX14 3DB, Abingdon, UK

[1]Association EURATOM - Belgian State, Laboratory for Plasma Physics Koninklijke Militaire School - Ecole Royale Militaire, TEC partner, 30 Avenue de la Renaissance B-1000 Brussels Belgium
** See annex of M.L. Watkins et al, "Overview of JET Results ", (Proc. 21st IAEA Fusion Energy Conference, Chengdu, China (2006)).*

Preprint of Paper to be submitted for publication in
Plasma Physics and Controlled Fusion

ABSTRACT.
The break-in-slope method is a simple - although powerful - data analysis technique that is commonly used to determine the power absorption profiles of the plasma species during auxiliary heating experiments in tokamaks. It is based on the study of the energy response of the particles to sudden changes in the external power applied to the plasma. Even though some experimental conditions are favorable for the straightforward application of the break-in-slope analysis in its most simple form (linear fit of the experimental temperature signals), most situations require the retention of additional terms in the linearized energy conservation equation for a successful use of this technique. These corrections include density and radiated power variations, the saturation of the temperature and density signals before and after the power break and the possible time delays between the power change and the energy response of the particles. The latter is particularly important for indirect (collisional) heating processes, while the other corrections play a crucial role in low absorption scenarios and/or single power step studies, where the standard break-in-slope analysis usually leads to integrated power levels well below the actual power injected into the plasma.

1. INTRODUCTION

All current-day tokamak experiments rely on auxiliary heating of the plasma particles for achieving high (fusion-relevant) temperatures. Up to now, the most promising heating schemes used in tokamaks involve two distinct processes: (i) the resonant (direct) heating of the particles by radio-frequency (RF) wave injection at the electron (ECRH) or ion (ICRH) cyclotron frequencies and (ii) the collisional heating of the particles by injection of high energy neutral particles (NBI). These methods have been extensively studied in various tokamaks worldwide and are foreseen for the International Thermonuclear Experimental Reactor (ITER) [1].

On top of the theoretical efforts to estimate the power deposition profiles of the various heating schemes by numerical modelling, there are various techniques used to infer the power absorption experimentally. Usually they are based on measurements of the electron/ion temperatures and densities. Amongst these methods, the break-inslope (BIS) and the Fast Fourier Transform (FFT) analyses of the experimental temperature responses to a discontinuity (or modulation) in the auxiliary powerapplied to the plasma have been systematically used in several tokamaks in the last years [2-6]. The FFT method requires, a priori, a periodic modulation of the external power and provides information on both the power deposition profiles and the diffusive / dissipative energy changes, being therefore very popular for transient transport studies [7-13]. The traditional break-in-slope technique does not distinguish between local power absorption and transport/losses, but has the advantage of requiring only a single discontinuity in the auxiliary power level to allow estimating the power absorption profiles. It is worthwhile mentioning that although the analysis of the experimental energy response of the plasma is, to a certain degree, independent of the specific nature of the heating mechanisms, the BIS/FFT methods have historically mainly been applied to radio-frequency heating scenarios, such as ECRH and ICRH experiments.

The common starting point for the BIS and the FFT analyses is a simplified version of the local energy conservation equation for a single non-collisional plasma species. The energy conservation equation for a given plasma species α can, to a first approximation, be written as [14]

$$\frac{\delta \varepsilon_\alpha}{\delta t} = \nabla \cdot (\kappa \nabla \varepsilon_\alpha + V \varepsilon_\alpha) + p_{aux} + \sum_j p_j - \frac{\varepsilon_\alpha}{\tau} \qquad (1)$$

where $\varepsilon_\alpha \equiv \varepsilon_\alpha(\rho, t) = {}^3/_2\, n_\alpha k_B T_\alpha$ is the local energy density of the species, n_α and T_α respectively being the local particle density and temperature, κ is the local diffusion coefficient, V is the convection velocity and p_{aux} is the auxiliary heating power density absorbed by the species in an infinitesimal volume element around the considered magnetic surface ρ). The sum Σp_j includes all other power sources in the energy equation (e.g. the ohmic power input) while the $\varepsilon_\alpha / \tau$ term represents the various local loss processes (e.g. radiation), where τ is a typical energy loss time arising from linearizing the equations and interpreting the sum of the various factors multiplying the energy as the inverse of an 'effective' loss time (in its most simple interpretation " is loosely identified with the energy confinement time τ_E).

This crude equation has the main ingredients to get a first rough idea of the fate of the power applied to the plasma: local energy increase or decrease either due to direct energy injection or loss, or through diffusion / convection. It is far from rigorous enough to capture detailed dynamics such as the energy flow between electrons and ions. Nevertheless, be it without offering a firm physical explanation, it will be demonstrated that it allows accounting for the majority of the power externally launched into the plasma when integrating the electron and ion power densities inferred from the plasma energy response. In spite of its simplicity, the equation will be stripped even further to isolate and highlight various individual effects one by one: starting from the simplest possible description (only retaining the auxiliary heating term in the above, assuming that all other phenomena happen on a much slower time scale than that imposed by the change in the auxiliary power), the impact of direct and – next - indirect particle heating on the temperature response will be studied first; then the effect of the density evolution will be added so that the full energy response to the power changes is looked at and not just the response of the temperature. The role of the loss term will be discussed in detail when further fine tuning the description of the particle responses to slow modulation or single auxiliary power steps, where the assumption that all phenomena that are not of interest happen on a longer time scale is easily violated. Finally, the importance of the proper definition of the "input power" will be looked into. In the present paper the accent is on local phenomena and diffusion and convection effects are deliberately left aside, i.e., no attempt is made to set apart the effect of the transport on the obtained energy response profiles from the actual local power deposition. A proper discussion of these effects – which displace energy (spatially) rather than simply adding or subtracting it locally - requires much more sophisticated tools [11-13], which distinguish external energy input from inflow from neighboring plasmas regions. The aim of the present paper is more modest: to check if the auxiliary power sent into the machine is indeed ending up in the plasma and to get a first guess of where it is found back.

This paper is organized following the steps just described to upgrade the usually adopted analysis for determining the power deposition profile of auxiliary heating to incorporate extra – and much needed but nevertheless in the literature largely discarded - effects. In section 2 an example of the classical break-in-slope analysis is presented and the main limitations of the standard method are illustrated. In section 3 we show how the BIS analysis can be extended to indirect heating regimes, by appropriately taking into account the time delays between the external power changes and the experimental plasma response signals. In section 4, we present an upgraded BIS analysis specially developed for the study of single power steps or slow modulation experiments. This involves the inclusion of several additional terms in the oversimplified energy conservation equation usually adopted in the classical BIS analysis in order to account for the slower changes in the plasma parameters in these time scales. After that, some applications of the improved method are shown, including a brief discussion on the importance of each term retained in the energy equation according to the particular situation studied. Finally, a brief summary followed by suggestions for further enhancement of the improved BIS method will be presented. Although all the applications of the upgraded BIS analysis introduced in this paper concern experiments performed in the JET tokamak, the main ideas and discussions are quite general and – provided the assumptions made here remain valid – the applicability of the presented data analysis technique to other experiments is straightforward.

2. THE STANDARD BREAK-IN-SLOPE

In many practical applications a periodic square wave modulation is imposed on the auxiliary power supplied to the plasma and the change in the slope of the energy density time evolution $\partial\varepsilon_\alpha/\partial t$ due to the power steps is used to infer the local power density absorbed by the particles. Assuming that the transport processes as well as the losses occur on a much longer time scale than the modulation period and discarding rapid variations of the other power sources, such as variations of the ohmic power caused by fluctuations of the plasma resistivity, the change in the slope of the local energy evolution $\partial\varepsilon_\alpha/\partial t$ due to a variation Δp_{aux}, in the locally dissipated power density can simply be written as [14]

$$\Delta \frac{\delta\varepsilon_\alpha}{\delta t} \approx \frac{3}{2} n_\alpha k_B \Delta \frac{\delta T_\alpha}{\delta t} \approx \Delta p_{aux} \tag{2}$$

where k_B is the Boltzmann constant and the local particle density $n_\alpha = n_0(\rho)$ is assumed not to vary significantly during the power step. This somewhat strong assumption is inspired on practical rather than fully justified physical arguments: fast measurements of the density profiles are not routinely available in most experimental set-ups. Moreover, it is important to mention that in most cases $\tau_{mod} < \tau_E$. rather than the stricter condition $\tau_{mod} << \tau_E$. As a consequence, heat diffusion and dissipative losses distort the constant $\partial T_\alpha/\partial t$ response, such that the absorption profiles determined with the standard BIS method do not fully mimic the shape of the actual power deposition. A more rigorous evaluation of the power absorption profiles – trying to set apart transport and losses from power deposition - would require additional sophistication in the data analysis (see e.g.–[12]). This is outside

the intended scope of the present paper. Indeed, as mentioned, eq.2 is based on the simplest possible form of the energy conservation equation for a single plasma species. Therefore it has to be applied very carefully, since the strong assumptions made above are only valid in limited conditions. For example, if the power modulation applied is not fast enough, processes that otherwise can safely be discarded may become important and the oversimplified energy equation no longer allows to capture the dominant physics. Furthermore, because of their different dynamics, electron and ion responses are quite different and thus require different modulation frequencies for a successful BIS analysis. Other important parameters are the density and the radiated power, which may change significantly during the power steps and in several cases have to be taken into account for satisfactory results. These corrections can become particularly important in low absorption efficiency scenarios or when the power step is large compared to the total external power applied to the plasma. Perhaps the most obvious drawback of the traditional BIS analysis is the fact that it is typically assumed that the temperature response of the plasma species is prompt to the external power change. This is certainly not always true, as for example in the case of the electron response in minority ICRH regimes, where a significant part of the RF power is first absorbed by the ions and afterwards transferred to the electrons by collisions.

As mentioned, in the standard BIS analysis one assumes a prompt linear response of the plasma temperature to the changes in the external power level. Hence, the temperature signals measured in various regions of the plasma are simply linearly fit during each semi-period of the modulation and the break in the (constant) temperature slopes $\partial T_\alpha / \partial t$ at each power step gives an estimate of the 'instantaneous' local power density variation Δp_{aux}. This is illustrated in Fig.1, where the electron temperature response (black) measured by one channel of the fast ECE radiometer at JET [15] to a square wave-modulation in the ICRF heating power (gray) is plotted together with the slopes obtained by linear regression of the temperature signals in three subsequent half-periods of the power modulation.

Note that in this particular example the change in the temperature response to the change in the external power applied is indeed practically instantaneous and that the modulation is fast enough to avoid the saturation of the local temperature due to diffusion/loss processes. Under such conditions, the standard BIS analysis based on the linear fit of the temperature signals at fixed time intervals imposed by the power modulation is clearly satisfactory. Consequently, it is not surprising that the BIS method has been successfully adopted to estimate the electron power absorption profiles in direct electron heating scenarios, such as ECRH [3,4] and modeconversion experiments [5,6].

However, for experiments with dominant ion-cyclotron heating of a minority species, commonly referred to as Minority Heating (MH) scenarios, the traditional BIS analysis of the electron response can not be applied as such, because in this regime most of the electrons are indirectly heated by collisions with the resonant ions near the IC resonance layer(s) and the electron temperature response is delayed with respect to the RF power change. Since this effect is usually not taken into account in the standard BIS analysis, the use of this technique in such conditions can lead to considerably underestimated values of the power absorption. Moreover, given that this collisional time delay is

different in each region of the plasma, even a fixed 'timeoffset' used in the standard BIS analysis to perform the temperature fit in a more appropriate time window would not be enough to correctly determine the electron power deposition profile over the entire plasma column.

To illustrate the differences in the electron responses due to the differing heating processes occuring in the plasma, Fig.2 shows examples of a 20Hz square-wave RF power modulation (gray curves) together with the corresponding electron temperature responses (black) measured with the ECE radiometer in typical mode-conversion MC (a) and minority heating MH (b) regimes in the JET tokamak. The two temperature signals correspond to the same ECE channel ($R \approx 3.15$m) registered in two different time intervals in an inverted (3He)H minority heating experiment (Pulse No: 63322), where a ramp-up of the ^{3}He concentration was performed to study the transition from the MH regime, for low [^{3}He], to the MC regime, for [^{3}He] > ~2% [16]. It is important to mention that the minority ion concentration corresponding to the MH to MC transition in the case of inverted ICRF heating scenarios is appreciably lower than in the standard heating case (with lighter minority), where typical values are around 10-15% [6]. The temperature traces shown in Fig.1 correspond to $T^*_e = T_{ECE} - \langle T_{ECE} \rangle_t$, i.e. the original ECE signal from which a smooth time-averaged temperature signal was subtracted. This operation is commonly done in the BIS analysis to remove the undesired slower variations of the temperature response. The amplitude of the RF power modulation (scaled in Figs. 2a and 2b) was approximately the same in both time intervals, namely, $RF\ \Delta P_{PRF} \approx 2.2$MW. The solid vertical lines indicate the time instants of the power modulation steps whilst the dashed ones indicate the approximate instants of the change in the temperature response (break-inslope instants) registered by the ECE radiometer in each case.

One clearly sees the almost instantaneous temperature response to the RF modulation in the MC regime (Fig.2a), whereas a time delay of roughly $\Delta t \approx 10$ms is needed for observing the change in the electron temperature slope in the MH case (Fig.1b), evidencing the nature of the indirect electron heating mechanism dominant in this regime. As mentioned, in this case the standard BIS method, which is based on the linear fitting of the experimental temperature signals in each half-period of the modulation (within solid lines), would include a sample of undesired data points in each time interval and therefore lead to wrong values of the temperature slopes and power densities. This is illustrated in Fig.3, where the RF power deposition profiles obtained with the standard BIS analysis in the MC (a) and in the MH (b) phases of Pulse No: 63322 are compared with the respective results obtained with the FFT analysis performed on the same time intervals. The absence of data near the plasma center is due to the fact that the JET fast ECE diagnostic system has a horizontal line-of-sight located ~15cm below the equatorial plane of the plasma [15]; the abscissae used in Fig.3 are not the major radii R at which the measurements are made but the radii corresponding to the same magnetic surface in the equatorial plane. The minority ion concentrations, estimated through charge exchange spectroscopy measurements [17], were respectively [^{3}He] ≈ 2.6% (a) and [^{3}He] ≈ 0.8% (b) in the snapshots corresponding to the MC and MH regimes represented in Fig.3 [16]. The gray box in Fig.3a indicates the region of predominant mode conversion heating in this discharge while the vertical dashed lines

indicate the cold IC resonance layer of the 3He ions, which is independent of the minority concentration.

As expected, in the mode-conversion regime (Fig.3a) the two methods produce very similar power absorption profiles, whereas in the minority heating regime (Fig.3b), where the electron response is delayed with respect to the RF power change, the BIS analysis breaks down. Note that the power density values obtained with the BIS analysis are completely wrong in the central region of the plasma (closer to the IC resonance layer), where the collisional energy exchange between the heated ions and the electrons is enhanced.

3. THE BREAK-IN-SLOPE PROCEDURE EXTENDED TO TIME DELAYS (BIS*)

In this section we present how to extend the standard break-in-slope technique to indirect heating scenarios, such as minority heating and NBI experiments. The method is based on the assessment of the actual break-in-slope instants observed in the experimental signals to establish the appropriate time intervals for computing the slopes of the temperature responses (i.e. the data points falling between the dashed rather than the full vertical lines in Fig.2). The maxima and minima of the temperature signals are statistically determined near all power steps in the various diagnostic (radial) channels, involving a careful processing of the experimental data. The automatic determination of the maxima/minima of the experimental signals is done in two steps: (i) First, the signals are filtered using a low-pass 2nd order Butterworth filter with cut-off frequency based on the diagnostics sampling rate and the modulation frequency, typically a few kHz for JET's ECE system; (ii) The time instants that correspond to the 3 largest (respectively lowest) values of the smoothed signals within an interval $t_0 + T/2$ to $t_0 - T/2$ around the break instants t_0 of the external power are registered. The average values of these triplets are then used as the break instants for the BIS* analysis at each power step. This procedure is applied to all diagnostic channels independently, as illustrated in Fig.4, where the filtered signals of 4 different ECE channels are shown. The dashed vertical lines represent the break instants determined by the improved BIS analysis routine while the solid lines represent the break instants of the power modulation.

It is clear that the accuracy in the evaluation of the break-in-slope instants is strongly dependent on the signal/noise ratio and the sampling rate of the experimental signals. Moreover, the presence of MHD activity (such as ELM's or sawtooth oscillations) in the plasma makes it virtually impossible to determine the experimental break instants fully automatically. Manual intervention is often required in such cases.

The performance of the new method has been assessed through benchmarking with the results obtained with FFT analyses on both direct and indirect electron heating experiments. As an example, Fig.5 shows a comparison of the electron power absorption profiles obtained in the already presented MC (a) and MH (b) phases of Pulse No: 63322 with three different methods: FFT analysis (□), standard BIS analysis (○) and improved BIS* analysis (▲). The power density values p_{RF} (shown per MW of the power modulation amplitude) represent the average of the values obtained in a time window of 0.2s starting at t = 8.6s (a) and t = 6.1s (b), respectively. The electron density measured

in the various channels of the Thomson scattering diagnostic (LIDAR) [18] available at JET were averaged during the 0.2s time intervals, and a high-order polynomial fit was applied to the time averaged density values in order to obtain smooth radial profiles for the calculation of the power absorption densities.

First note the very good agreement between the power absorption profiles obtained with the three different methods in the mode-conversion case (Fig.5a), where the break instants used by the BIS* routine practically agree with the RF power breaks used by the standard BIS analysis. In the minority heating regime (Fig.5b), as shown before, the standard break-in-slope method leads to totally underestimated power density values in the indirect electron heating region (R < 3.3m) while the power deposition profile obtained with the corrected break instants (BIS*) nearly agrees with the FFT result. The small differences between the FFT and the BIS* results may be related to the fact that only the fundamental (N=1) deposition profile of the FFT analysis is shown in Fig.5 (i.e., the profile obtained from a sinusoidal temperature response to the launched power at the modulation frequency). The BIS* result, on the other hand, contains information of the complete response spectrum, since it is based on the linear fit of the nearly 'triangular' temperature response signals to the actual square wave modulation (with infinite Fourier spectrum) imposed in the RF power.

As pointed out before, the FFT analysis automatically accounts for the time delays in the plasma response, since the experimental signals are represented in terms of their Fourier amplitude(s) and phase(s). As illustrated in Fig.6 for the minority heating phase of Pulse No: 63322 represented in Fig.5b, the time delays determined by the upgraded BIS* procedure show a clear correlation with the phases obtained by the FFT analysis.

First note the gradually increasing time delays observed near the plasma center, reaching values of $\Delta t \sim 12$ms, roughly one fourth of the RF modulation period (50ms). This feature clearly indicates a region of predominant indirect electron heating, where the wave energy is first absorbed by the resonant ions around their IC resonance layer (R- 2.98m) and afterwards transferred by collisions to the electrons.

The minimum observed around R≈3.4m in Fig.6, indicating a region of direct electron heating in the MH regime, deserves a few additional words. Detailed numerical modeling of this inverted ICRH scenario using the full-wave code CYRANO [19] has shown that the presence of small traces of Carbon and Deuterium in the discharge gave rise to a parasitic mode-conversion layer at the high-field side of the plasma, near $R \approx 2.6$m. Recalling that the plasma magnetic axis is around $R \approx 3.0$m in this experiment, we see that the reduced values of the heating time delays detected around $R \approx 3.4$m are fully consistent with the direct electron heating on the magnetic surfaces associated to the new MC layer theoretically predicted.

Perhaps the main advantage of the BIS* technique with regards to the FFT is the fact that it, in principle, only requires a single discontinuity in the auxiliary power level for its application. Equivalently, in modulation experiments the extended BIS* analysis provides, by definition, 'instantaneous' information on the power density profiles and the heating time delays at each power step, which is particularly interesting when studying discharges with heating regime transitions. This

is illustrated in Fig.7, where the electron power absorption profiles estimated with the BIS* analysis in consecutive time intervals of Pulse No: 63322 are plotted. One can clearly see the evolution of the power absorption as function of the increasing minority concentration (represented in the inset): starting from relatively low power densities with a maximum around the IC resonance layer ($R \approx 3.0$m) in the beginning of the discharge (MH regime) and culminating with higher power density values with a maximum absorption slightly shifted off-axis ($R \approx 3.15$m) for higher 3He concentrations (MC regime). The location of this maximum is in good agreement with theoretical predictions of the mode-conversion layer position for the corresponding ^{3}He concentration, as depicted in Fig.5a. The integrated power fractions absorbed by the electrons obtained in the MH (●) and in the MC (▲) regimes in this case were respectively 25% and 65%.

The presented example clearly demonstrates that considering the actual time instants at which the local temperature slopes 'break' extends the applicability of the break-in-slope technique to indirect heating scenarios, a regime that can not properly be diagnosed with the traditional BIS analysis.

4. THE BIS ANALYSIS FURTHER EXTENDED TO SLOW MODULATION OR SINGLE POWER STEPS

Up to now we restricted ourselves to examples involving the determination of the power deposition profiles in experiments in which the modulation frequency of the external power was deliberately chosen to be high enough to avoid a major influence of transport / loss processes in the local experimental responses. In many experiments, however, the auxiliary power applied to the plasma is not modulated. The BIS analysis then allows determining the power absorption profile if there is at least one power step (a switch-on/off of the external power source) during the 'flat-top' of the discharge. In these cases, however, several plasma parameters may also change in a timescale comparable to the energy variations and the analysis of the plasma response to the change in power can no longer be considered to be a perturbative technique. The same holds true if the modulation applied to the external power is slow compared to the transport and/or dissipative processes in the plasma. As a consequence, to successfully apply the BIS analysis in such conditions, supplementary physics needs to be retained when simplifying the energy conservation equation. As will be shown, the most important terms to be included are the density variations, the saturation of the temperature and density signals after the power step and the change in the power lost by radiation.

The inclusion of density variations has historically been neglected in the BIS/FFT analyses in most tokamak experiments because of the unavailability of simultaneously time and space resolved density measurements. In the case of JET for example, the Thomson scattering measurements (LIDAR) have a good spatial resolution (50 channels) but only a modest time resolution (250ms), making it impossible to properly analyze the density evolution after the change in the external power level. The fast interferometer diagnostics (KG1) [20], on the other hand, has a relatively high sampling rate (10ms) but has only 4 horizontal and 4 vertical channels, making the reconstruction of the density profiles rather challenging.

As a first approximation, we can upgrade the BIS analysis by adding the density's temporal response to eq.2 in order to not only account for the time dependent temperature $T_\alpha = T_\alpha(t)$ but also for the density $n_\alpha = n_\alpha(t)$ variations:

$$\Delta \frac{\delta \varepsilon_\alpha}{\delta t} \approx \frac{3}{2} k_B \left(n_{0\alpha} \Delta \frac{\delta T_\alpha}{\delta t} + T_{0\alpha} \Delta \frac{\delta n_\alpha}{\delta t} \right) \approx \Delta p_{aux} \qquad (3)$$

Here $n_{0\alpha}(\rho)$ and $T_{0\alpha}(\rho)$ are the local values of the temperature and density of the studied species evaluated at the power break, respectively. Because of the lack of temporally resolved density profile measurements, the density slopes $\partial n_\alpha / \partial t$ before and after the power step are inferred from the line integrated (fast) interferometer signals and these slopes are used to represent the time evolution of the local plasma densities measured with the (slow) LIDAR system.

In Fig.8a the lines-of-sight of the eight channels of the fast interferometer diagnostics (KG1) are represented together with a schematic cross section of the JET tokamak. An example of the determination of the slopes in one of the KG1 signals (channel 3) is presented in Fig.8b while the values of the normalized density slopes evaluated after the power break in all KG1 channels are depicted in Fig.8c. The averaged value of the normalized slopes computed from several KG1 channels (dashed line in Fig.8c) is used as reference to describe the evolution of the local densities $n_\alpha(t)$ close to the auxiliary power step. The signals from channels 1 and 4 (hollow circles in Fig.8c) are typically discarded from the analysis, since they mostly reflect the edge density of the plasma and their response to the change in the external power applied is usually faster than that of the core, where the dominant heating takes place for the studied scenarios.

The saturation of the local temperature and density signals due to diffusion / loss processes must also be considered when applying the BIS analysis to single or slowly modulated power steps. To some extent, these effects can be accounted for by dropping the assumption that " is large and retaining only the effect of the simplified loss term $-\varepsilon_\alpha/\tau$ in the right-hand side of eq.1. This leads to exponential (instead of linear) solutions of the local energy evolution that can be written as

$$\varepsilon_\alpha(\rho, t) = \varepsilon_{0\alpha} e^{-\frac{(t-t_0)}{\tau_\alpha}} + A_\alpha ¥ (1 - e^{-\frac{(t-t_0)}{\tau_\alpha}}) \qquad (4)$$

where $\varepsilon_{0\alpha}(\rho) = {}^3/_2\, n_{0\alpha} k_B T_{0\alpha}$ is the local energy density at the break instant ($t = t_0$) and $A_\alpha(\rho)$ and $\tau_\alpha(\rho)$ are the adjusted parameters determined by minimization of the experimental signals. The time parameter $\tau_\alpha(\rho)$ represents the characteristic energy loss time of the species ! in each region of the plasma while the parameter $A_\alpha(\rho) = \Delta p_{aux}\, \tau_\alpha(\rho)$ depends on the magnitude (and sign) of the power change.

Both diffusion and loss processes affect the experimental measurements of the local temperatures and densities. The loss term $(-\varepsilon_\alpha/\tau)$ included in the right-hand side of the energy equation does capture the behaviour of the experimental signals satisfactorily but it can not directly be related to one individual physical phenomenon.In this sense, the adjusted time parameter $\tau_\alpha(\rho)$ reflects

the *ensemble* of transport and loss effects on the local measurements of the temperature / density of the studied species.

In practice, the temperature and density signals are individually (rather than as a product ε_α) fit by exponential functions of the form of eq.(4) before and after the power step, and the break in their time derivatives ($\Delta\partial T_\alpha/\partial t$, $\Delta\partial_\alpha/\partial t$,) near the power step is evaluated analytically from the adjusted parameters. Afterwards, the two contributions are added according to eq.3 to provide an estimative of the local power density variation $\Delta p_{aux}(\rho)$.

The exponential representation of the experimental signals has shown to be particularly important for correctly computing the temperature/density slopes after the auxiliary power step, where the time derivatives of the signals may vary relatively fast and the analysis in terms of a linear fit would require too small time intervals for a statistically relevant minimization. Before the power step, on the other hand, the linear and exponential fits usually lead to similar temperature and density slopes, because in most cases the plasma has practically reached stationary condition and the magnitude of the $\partial/\partial t$ derivatives are small.

In Figure 9 we show examples of the linear and exponential fits applied to one of the charge-exchange (KS5) ion temperature signals in JET [17] registered during an RF power step of ~1.5MW (see inset). The dotted lines represent the time derivatives obtained from the exponential fit near the power break while the dashed lines show the linear slopes. The thin vertical lines indicate the time intervals used for each minimization procedure.

First note that the time interval for the linear fit following the power step has been chosen smaller than the one for the exponential fit, in order to reduce as much as possible the influence of the signal saturation in the former. The minimum time intervals for the linear fit are limited by the signal/noise ratio and the sampling rate of the diagnostic signals. For the exponential fit, on the other hand, longer time windows lead to even more accurate determination of the adjusted parameters and signal slopes after the power break. Also note that, as mentioned, the linear and exponential minimizations applied before the power break lead to very similar results, while after the break the time derivative of the exponential function is significantly larger than the one obtained with the linear fit. Naturally, in the single power step or slow modulation cases, the determination of the correct break instants to perform the exponential minimization on each temperature/density channel also plays an important role for the successful application of the method.

Finally, another important ingredient for a more reliable interpretation of the BIS results on single or slowly modulated power steps is the consideration of the changes in other power sources/ sinks in the plasma. Although small changes in the Ohmic power always occur in these situations due to variations of the plasma resisitivity, Z_{eff}, etc., the dominant effect seems to be related to the changes in the radiated power. For example, it is well known that the application of high levels of ICRF power in tokamaks is followed by an increase of the power radiated from the plasma. This is not only related to the heating of the plasma species and the resulting increase in the Bremstrahlung radiation, but predominantly due to the change of the edge properties and the plasma impurity

content associated with the ICRF application, which may cause a considerable augmentation of the impurity line emission particularly in the outer regions of the plasma ($\rho > 0.5$). That is, in the cases where the radiated power varies noticeably during the applied power step, the absorption profiles determined by the BIS analysis do not represent solely the auxiliary power absorbed by the plasma species, but actually the combination of the locally absorbed and radiated power densities $\Delta p_{aux} + \Delta p_{rad}$. Since the changes in the radiated power are often relatively fast, a careful consideration of this effect would require the Abel inversion of soft Xray and/or bolometer signals in a very fine temporal grid, which would make the analysis much more time-consuming. A first order correction can be made, though, by subtracting the change in the total radiated power measured by the bolometers from the change in the external power applied to the plasma, i.e., by considering that the effective power step is given by $\Delta(P_{aux} - P_{rad})$, instead of Δp_{aux}, in the normalization of the BIS results. To illustrate this effect, in Fig.10a we show an example of the time traces of the neutral-beam (NBI), ion-cyclotron (ICRF), ohmic (OH) and radiated (RAD) power values measured in Pulse No: 68733 at JET, where the RF power was switched off between t = 9s and t = 10s. In Fig.10b, the effective power change during the RF switch-off phase when either including or omitting the radiated power correction is depicted. As it is not significantly affected, the ohmic power input has been neglected in the determination of the power steps represented in Fig.10b.

Note that because of the decrease in the radiated power level in the phase without ICRF, the effective power step is considerably lower than the initially believed value of approximately 1.5MW. Likewise, in the ICRF switch-on, at t = 10s, only about 1MW of the 1.5MW of RF power is effectively being transferred to the plasma, since roughly 0.5MW of the power applied is 'immediately' radiated. Although clearly nonnegligible, this effect has commonly not been accounted for in the interpretation of the power deposition profiles estimated from modulation experiments in the past. The radiation corrections depend strongly on the type of auxiliary power studied (ECRF, ICRF or NBI), and particularly on the absorption efficiency of each heating mechanism. In the case of ICRH, for example, the lower the absorption efficiency of the heating regime the most important this correction may become, since for low single-pass absorption scenarios the RF power keeps sloshing around and the plasmawall interactions are usually more pronounced, leading to a higher impurity content and consequently larger radiation losses in the plasma.

Taking into account the variations of density and radiated power together with an exponential time dependence of both temperature and density responses helps to further improve the break-in-slope analysis, in particular when the auxiliary power change is large and slowly modulated (perturbative experiments). This will appear very clearly in the next section, where different examples are treated.

5. APPLICATIONS TO TYPICAL JET DISCHARGES

As a first application of the improved BIS procedure let us consider the analysis of the switch-off of the RF power in a Deuterium majority ICRH experiment performed at JET [21]. This heating scenario is characterized by a low single-pass absorption efficiency making the corrections discussed in the

previous section essential for a reliable evaluation of the RF power deposited in the plasma. Moreover, in this experiment all relevant diagnostics for a complete BIS analysis were available - fast ECE (KK3) and charge-exchange (KS5), interferometer (KG1) and Thomson scattering (LIDAR), bolometry - making it possible to estimate the power absorption profiles for both ions and electrons simultaneously and compare the (integrated) results with the nominal injected RF power calculated from the antenna impedance measurements.

In Fig.11 we show the time traces of the ion (a) and the electron (b) temperatures obtained respectively with the charge-exchange (KS5) and fast ECE (KK3) diagnostics at JET during a $\Delta t = 1s$ switch-off of the ICRF power in Pulse No: 68733. The RF power step corresponds to the case represented in Fig.10, i.e., to a power 'well' of approximately 1.5MW. When considering the decrease in the radiated power during the RF shut down phase, the effective power step is around 1MW.

To discuss in detail the importance of the various terms retained in the simplified energy equation (eq.1), the BIS analysis was applied with 4 different minimization procedures: (i) linear T_α fit with constant density n_0 (standard BIS); (ii) exponential T_α fit with constant n_0; (iii) linear T_α and n_α fits; (iv) exponential T_α and n_α fits. The power absorption profiles obtained with the improved BIS analysis at the ICRF power step ($t = 9s$) for the ions (a) and for the electrons (b) with the various combinations described above are shown in Fig.12. Similar time intervals for the linear ($\Delta t \approx 0.2s$) and exponential ($\Delta t \approx 0.5s$) minimizations of the experimental signals were used for both computations. Note that in the case of the electrons, however, the temperature signals near the plasma edge suffer a slight increase right after the RF switch-off, to afterwards enter the expected relaxation phase. This small increase, which has been discarded in the BIS analysis of the T_e signals, is related to the reduction of the impurity level in the plasma following the RF shut down.

First note the large difference between the linear and the exponential fit in the ion temperature analysis for the constant n_0 results (○,●), as opposite to the electrons case, where the decay of the T_e signals is smoother (see Fig.11b) and the linear and exponential representations of the temperature lead to very similar results except near the plasma center. The density corrections play a crucial role in both cases, being even more prominent in the electron analysis, where the $\partial T_e/\partial t$ contribution to the energy slope is smaller. The exponential description of the density and temperature evolution leads to the highest power density values in both cases, while the omission of the density variations leads to strongly underestimated power absorptions. In this example, the exponential description (■) provides local power density values as high as ~3 times (for ions) and ~5 times (for electrons) the values obtained with the classical BIS method (○), where a constant density n_0 and linear T_α evolution is considered.

To further illustrate the importance of the various minimization procedures in the BIS analysis, the cumulative power levels $P(\rho) = \int_r^0 p_{RF}\, dV$ corresponding to the absorption profiles shown in Fig.12 are represented in Fig.13. The integrated power values are normalized to the total auxiliary power step of $\Delta P_{aux} = 5.1$MW.

Note that in the case of the exponential representation of the temperature and density signals (■),

about 40% (ions) + 25% (electrons) ≈ 65% of the ΔP_{aux} = 1.5MW RF power change is recovered with the BIS analysis. This is consistent with the effective power change of $\Delta P_{aux} \approx$ 1.5MW obtained when considering the global radiation corrections in the total power applied. Moreover, wave absorption near the plasma edge and/or in the scrape-off layer (which is not in the line-of-sight of the diagnostics and therefore is not captured in the data analysis) also contributes to the underestimation of the integrated power levels with respect to the total applied external power (inferred from antenna impedance measurements in the case of ICRH). In the worse case, the standard (linear) BIS analysis with constant density (○), only ~17% (~0.25MW) of the nominal ICRF power is obtained when integrating the estimated power profiles. Even the exponential description of the temperature evolution with constant density (●) is not sufficient to successfully describe this case, giving roughly ~25% (~0.4MW) of the nominal power removed from the plasma.

An alternative way to apply the improved BIS analysis with the density corrections is to combine the experimental temperature profiles measured with the ECE/CX diagnostics with the time-resolved density profiles reconstructed from the combined LIDAR/interferometer measurements, and perform a single fit on the resulting energy density signals $\varepsilon_\alpha(\rho, t) = n_\alpha(\rho, t) \cdot T_\alpha(\rho, t)$. Besides being more time consuming than the method based on the independent evaluations of the $\partial T_\alpha/\partial t$ and $n_\alpha(\rho, t)$ slopes, this approach is more sensitive to eventual differences in the time delays between the temperature and density responses to the break in the power level. In Fig.14a we compare the power absorption profiles obtained for the ions and electrons with the analysis of the convoluted $\varepsilon_\alpha(\rho, t) = n_\alpha$ signals (hollow symbols) with the results obtained with the independent $T_\alpha(\rho, t)$, $n_\alpha(\rho, t)$ exponential fits (full symbols) already shown in Fig.13. In Fig.14b the corresponding (normalized) integrated power levels are depicted.

Note that in the case of the ions the two methods lead to virtually the same results, whereas for the electrons, the method based on the analysis of the convoluted energy profiles (□) provides systematically lower power density values throughout the plasma. This is explained by the fact that the break instants considered in the T_e signals are delayed with respect to the break instants used in the analysis of the interferometer density signals. In the independent dT_e/dt, dn_α/dt calculation, this has no influence because the time delays are individually accounted for and the two components of the total energy derivative are simply added together (eq.3). However, since the analysis of the convoluted n_eT_e signals is done using the break instants determined from the ECE measurements (where the local densities have already started to change), the density corrections are slightly underestimated. For the ions, this effect is much smaller because in most cases the T_i and the density signals are practically in phase.

The results of the improved BIS analysis of various ICRH experiments performed at JET have been frequently cross-checked against simulations using the full-wave code CYRANO [19]. In several cases, including the one just presented, the power absorption profiles obtained with the upgraded BIS method are in relatively good agreement with the theoretical predictions [22]. Nevertheless, the experimental power deposition profiles are typically broader than the ones predicted numerically,

what is consistent with the fact that the experimental data analysis inevitably embeds transport and loss effects, while the theoretical profiles estimated with the CYRANO code simply represent the non-collisional RF wave absorption processes.

Another example of the application of the improved BIS analysis is the evaluation of the power absorption of the fast NBI ions injected in a (^{3}He)D type-III ELMy H-mode experiment in JET (Pulse No: 69388). In this pulse, approximately 18MW of mixed 80keV/130keV Deuterium beam power and 4MW of ICRF power were applied throughout the flat-top of the discharge. Lower-hybrid preheat was used during the formation of the plasma to retard the current diffusion and avoid sawteeth activity during the main phase of the discharge. Two diagnostic beams (~3MW) were maintained after the high power NBI switch-off to allow ion temperature and plasma rotation measurements via active charge exchange spectroscopy. This scenario is illustrated in Fig.15a, where the time traces of the neutral-beam (NBI), ion-cyclotron (ICRF), ohmic (OH) and radiated (RAD) powers registered near the end of Pulse No: 69388 are plotted. Note that even with almost 15MW of NBI power being removed from the plasma at t = 50s, the radiated power only starts decreasing ~100ms afterwards and even then, the decay is relatively smooth. This suggests that in the NBI case, the corrections due to radiation changes in the BIS analysis are less important than in the case of the ICRF power break discussed before. This can be seen in Fig.15b, where the effective auxiliary power steps when including or omitting the total radiated power measurements are depicted. Because of the delay in the *Prad* decay, the effective power step with and without the radiation corrections are practically the same near the break instant, namely $\Delta P_{aux} \approx$ 15MW. It is important to mention, though, that the gradual decrease of about 4MW in the total radiated power during the 500ms following the NBI switch-off is not totally negligible. The temperature and density signals will naturally include this effect and the adjusted parameters (A, τ) of the exponential decay of the experimental signals will reflect de actual power level evolution and not the constant power level assumed initially. The delay in the P_{rad} decay with respect to the NBI switch-off was systematically observed during this campaign, and is believed to be related to the presence of impurities that were injected during the experiments.

The time traces of the ion and electron temperature measurements used to perform the BIS analysis to the NBI power step (t = 10s) in Pulse No: 69388 are illustrated in Fig.16a and Fig.16b, respectively. Note that even though the ion and electron temperatures start to decrease after the ~4MW of ICRF power was removed from the discharge (t = 9.5s), the plasma has practically achieved thermal equilibrium when the NBI power is switched-off (t = 10s).

Note that the ion response is nearly concomitant with the NBI power change, while the electron temperature response is slower. Some of the 'central' ECE channels even show a small increase of the local T_e values just after the NBI switchoff before entering the relaxation phase. This should not be confused with the increase observed in the peripheral T_e signals following the switch-off of the ICRF power discussed before, where the effect is connected to the impurity level close to the plasma edge. In the NBI case, the increase observed in some of the ECE channels is related to the so called Post Beam Pulse effect [23], a typical feature of the NBI physics related to the sudden interruption of the

cold electrons injection (originating from the ionization of the neutral beam) that leads to a temporary electron temperature rise following the shut-down of the beam power in certain regions of the plasma.

The power absorption profiles obtained for the ions (a) and for the electrons (b) in the NBI switch-off analysis of Pulse No: 69388 obtained with the 4 different approaches discussed before are compared in Fig.17: (i) linear T_α fit with constant density n_0 (standard BIS); (ii) exponential T_α fit with constant n_0; (iii) linear T_α and n_α fits; (iv) exponential T_α and n_α fits. The power densities are normalized to the NBI power step of $\Delta P_{aux} \approx 15$MW.

Similar to the ICRF case, it is clear that the approach based on the exponential description of the temperature and density signals provides considerably larger power absorption values than the other methods. Even the shape of the profiles obtained with the linear analyses differs significantly from those obtained with the exponential minimization in this case. Note that for the ions, the exponential fit of the temperatures signals plays the main role in the evaluation of the power absorption profiles while for the electrons, the density corrections and the exponential descriptions have similar weights on the final calculation of the absorption profiles.

The total integrated power levels corresponding to the profiles shown in Fig.17 are depicted in Fig.18.

As in the previous example, only the analysis based on the exponential description of the experimental signals (■) provides integrated power levels compatible with the nominal value of the NBI power removed from the plasma. In this case, 50% (ions) + 35% (electrons) = 85% of the $\Delta P_{aux} \approx 15$MW power step is obtained after the integration of the power absorption profiles. In the case of the standard BIS results (○), only ~35% (~5MW) of the total NBI power is recovered, showing once more that the simplified procedure is not at all suited for the study of large power steps (strongly perturbative experiments). As mentioned before, one possible reason for the slightly underestimated power level found in this case with the upgraded BIS analysis is the fact the adjusted parameters do include the decay of the radiated power after the NBI power switch-off and therefore reflect a somewhat lower effective power step. Other factors like the restricted line of sight of the measurements, beam shine through effects, etc., are likely to also influence theresults.

In most of the examples studied, the power fractions absorbed by the ions and the electrons by the NBI ions are in qualitative agreement with the PENCIL code [24] calculations. Once more, the experimental power absorption profiles are usually broader than the numerical ones, particularly for the electrons. Here also, transport effects and losses that are eventually not included in the PENCIL calculations but are inevitably captured with the BIS analysis of the experimental signals may be a strong contributor to these differences.

SUMMARY AND DISCUSSION

An improved data analysis technique for estimating the power absorption profiles of auxiliary heating schemes in tokamak plasmas was presented. It is based on the Break-In-Slope (BIS) method and exploits the experimental response of the plasma energy to sudden changes in the external power applied to infer the local power densities absorbed by the plasma species. In the classical BIS analysis

one typically considers that the plasma temperature response to the external power change is the dominant mechanism, discarding e.g. density or radiated power variations. Moreover, it is assumed that the temperature varies much faster than the other physical processes responding to the change in the power level, such as transport and loss effects, and the temperature evolution around the power step is naively described by a linear function of time. Because these assumptions are only valid in limited circumstances, the successful application of the BIS analysis was, up to now, constrained to 'nonperturbative' heating experiments, that is, to experiments with rather fast power modulations and moderate amplitudes [3-6]. When larger perturbations of the plasma parameters result from the discontinuity in the power applied, the BIS immediately breaks-down and a more sophisticated analysis of the experimental signals is needed.

Several upgrades were necessary to extend the applicability of the classical BIS method to more general cases: the consideration of the time delays observed between the temperature responses and the applied power, the inclusion of the density variations resulting from the power changes, the retention of a simplified loss term in the energy equation to account for the saturation of the temperature and density signals due to loss/transport processes and the consideration of the variations of the radiated power. The importance of each of the phenomena mentioned above strongly depends on the heating scenario, on the perturbation amplitude and frequency, and on the plasma species studied. The procedure presented here includes all the cited corrections and is therefore suited to analyze a large variety of heating scenarios:

- In indirect heating regimes, the time delay correction has shown to play a crucial role, as was illustrated with the analysis of a (fast) modulated ICRF minority heating experiment in JET;
- For slow modulation or single power step experiments, the additional inclusion of the density variations and the loss term demonstrated to be essential;
- For low absorption scenarios or perturbative experiments (large power steps) the radiated power has additionally to be accounted for;

These combined effects were demonstrated through the analyses of two single power step experiments: a low-absorption minority ICRH scenario and a high power NBI switch-off. In both cases, all the ingredients mentioned above had to be included in the analyses for obtaining integrated power levels compatible with the nominal power values injected in the plasma by the respective auxiliary heating systems. On the other hand, the application of the classical BIS technique to these cases led to severely underestimated power levels deposited in the plasma.

Besides providing integrated power values compatible with the experimental measurements of the power launched into the plasma, the power absorption profiles estimated with the upgraded procedure presented are often very different from the profiles obtained with the classical (linear) BIS analysis. By fine-tuning the description of the time evolution of the experimental signals and properly dealing with the time delays between the several measured quantities and the power modulation, the power deposition profiles may reveal additional structures related to secondary absorption mechanisms in the plasma, that would otherwise be overseen with the classical BIS approach.

Various enhancements may still be included in the upgraded BIS analysis to obtain even more trustworthy evaluations of the power deposition profiles. Perhaps the most obvious improvement would be a more detailed description of the local density evolution, based either on direct time-resolved measurements of the particle density profiles or on the numerical inversion of the existing - but unfortunately lineintegrated rather than local – fast interferometer signals. Similarly, the radiation profiles could be included via the inversion of the bolometer and soft X-ray signals, allowing one step further in the discrimination between actual power deposition and losses in the results of the analysis.

ACKNOWLEDGEMENTS

The authors would like to thank the whole JET team, in particular the diagnostics group for fruitful discussions on the limitations and uncertainties of the experimental measurements and the careful processing of the experimental data used in this work.

REFERENCES

[1]. ITER team *et al*., *"ITER Physics Basis"*, *Nucl. Fusion* **39**, p.2137 (1999).
[2]. Gambier D. J. *et al*., *Nucl. Fusion* **30**, p.23 (1990).
[3]. Kirov K.K *et al.*, *Plasma Phys. Control. Fusion* **44**, p.2583 (2002).
[4]. Leuterer F. *et al., Nucl. Fusion* **43**, p.744 (2003).
[5]. Lin Y. *et al., Plasma Phys. Control. Fusion* **45**, p.1013 (2003).
[6]. Mantsinen M.J. *et al., Nucl. Fusion* **44**, p.33 (2004).
[7]. Gorini G. *et al., Phys. Rev. Lett.***71**, p.2038 (1993).
[8]. Lopes Cardozo N.J. *et al., Plasma Phys. Control. Fusion* **37**, p.799 (1995).
[9]. Imbeaux F. *et al., Plasma Phys. Control. Fusion* **43**, p. 1503 (2001)
[10]. Ryter F. et *al., Nucl. Fusion* **43**, p.1396 (2003).
[11]. Mantica P. *et al., Plasma Phys. Control. Fusion* **44**, p.2185 (2002).
[12]. Mantica P. *et al*., *Phys. Rev. Lett.* **96**, 095002 (2006).
[13]. Marinoni A. *et al., Plasma Phys. Control. Fusion* **48**, p. 1469 (2006).
[14]. Van Eester D, *Plasma Phys. Control. Fusion* **46**, p.1675 (2004).
[15]. de la Luna E. *et al., Rev. Sci. Instrum.* **75**, p.3831 (2004).
[16]. Mayoral M.-L. *et al., Nucl. Fusion* **46**, p. 550 (2006).
[17]. von Hellermann M. G. *et al*., *Rev. Sci. Instrum.* **61**(11), p.3479 (1990).
[18]. Saltzmann H. *et al., Rev. Sci. Instrum.* **59**, p.1451 (1988).
[19]. Lamalle P. U., *LPP-ERM/KMS Lab. Report* **101**, Brussels (1994).
[20]. Braithwaite G. *et al., Rev. Sci. Instrum.* **60**, p.2825 (1989).
[21]. Krasilnikov A. *et al.*, "*Ion cyclotron resonance heating of JET deuterium plasmas at the fundamental frequency*", to appear in AIP Conf. Proc. of 17th Topical Conference on RF Power in Plasmas, Clearwater (2007).

[22]. Lerche E.A. et al., "*D majority heating in JET plasmas: ICRH modelling and experimental RF deposition*", to appear in AIP Conf. Proc. of 17th Topical Conference on Radio Frequency Power in Plasmas, Clearwater (2007).

[23]. Eubank H. *et al., Conf. Proc. of 7th IAEA Conference on Plasma Physics* 1, p.167, IAEA Innsbruck (1978).

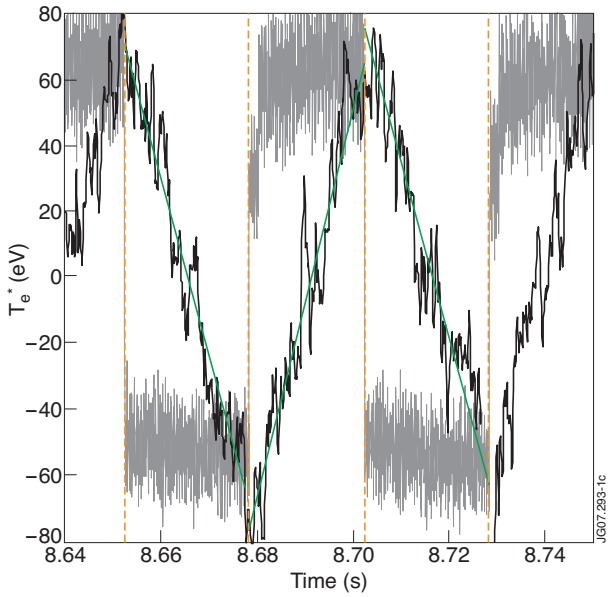

Figure 1: Example of the classical break-in-slope method illustrating the linear fit of the electron temperature signal (black) applied in consecutive half-periods of the power modulation (gray).

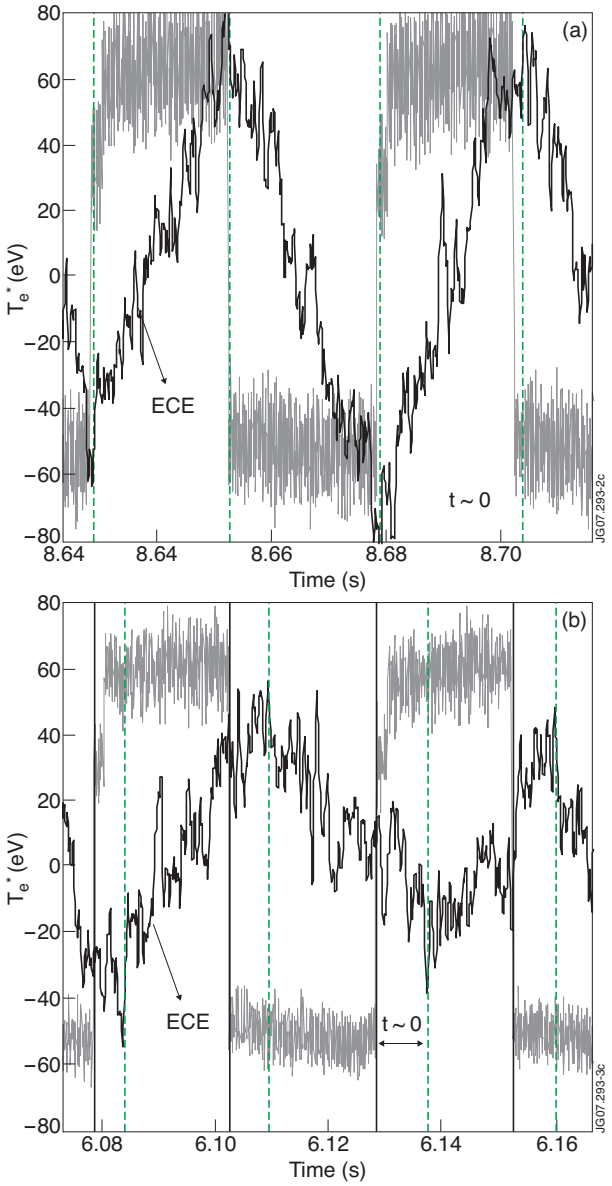

Figure 2: Examples of the electron temperature responses (ECE) used for the break-in-slope analysis in typical MC (a) and MH (b) heating scenarios in JET. Note the clear time delay ,t observed in the temperature response with respect to the RF power modulation (gray curve) in the MH regime (b), a typical signature of the indirect heating of the electrons.

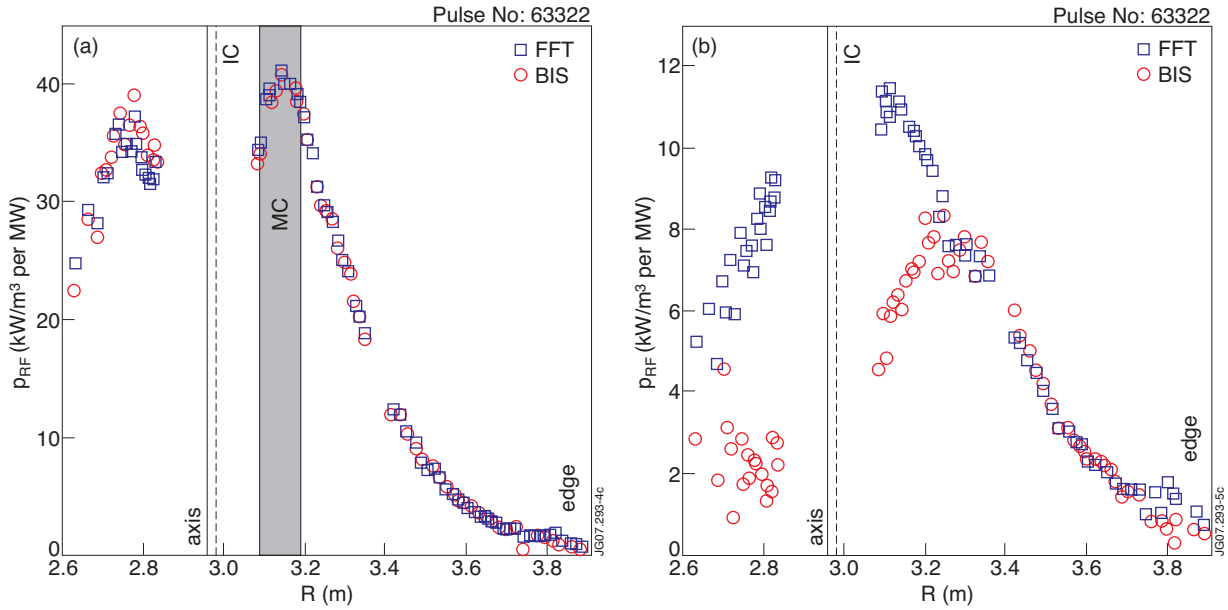

Figure 3: Electron power absorption profiles obtained with the standard BIS analysis (○) and the FFT analysis (□) of the ECE signals in the mode-conversion (a) and minority heating (b) phases of Pulse No: 63322, evidencing the failure of the standard BIS method when indirect (collisional) heating of the electrons is the dominant mechanism.

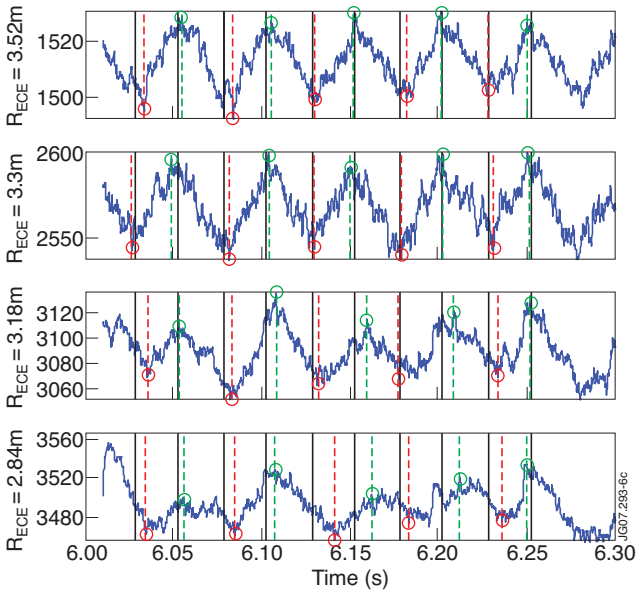

Figure 4: Example of the automatic determination of the break-in-slope instants performed by the extended BIS routine on 4 ECE channels.

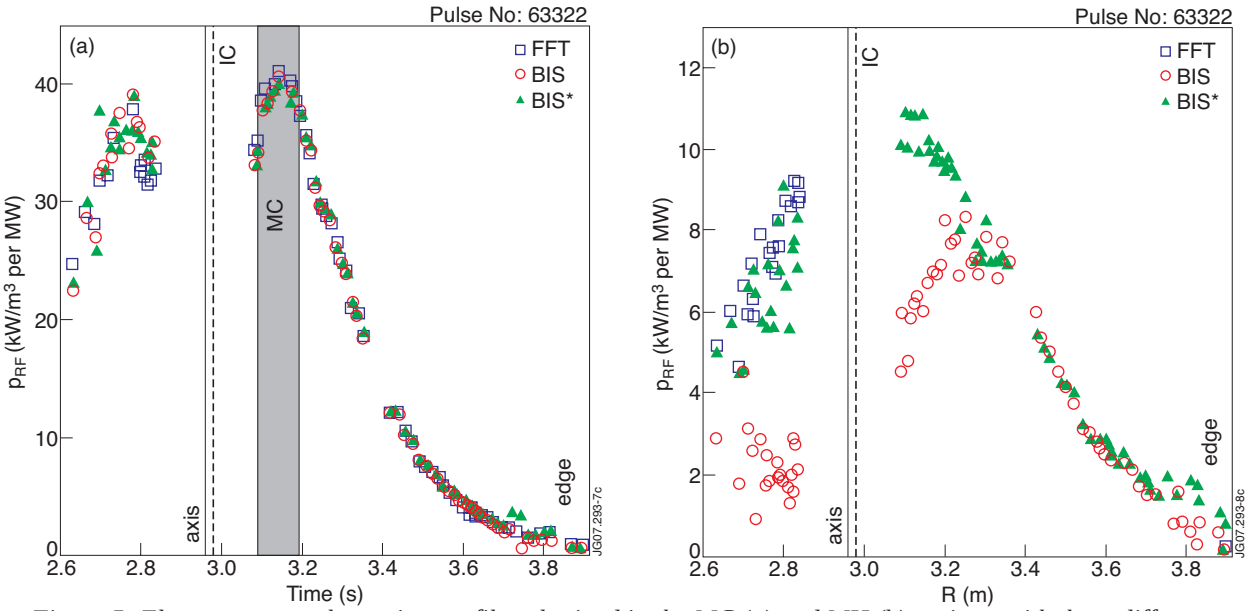

Figure 5: Electron power absorption profiles obtained in the MC (a) and MH (b) regimes with three different methods: (N=1) FFT analysis (□), standard BIS analysis (○) and extended BIS analysis (▲)*

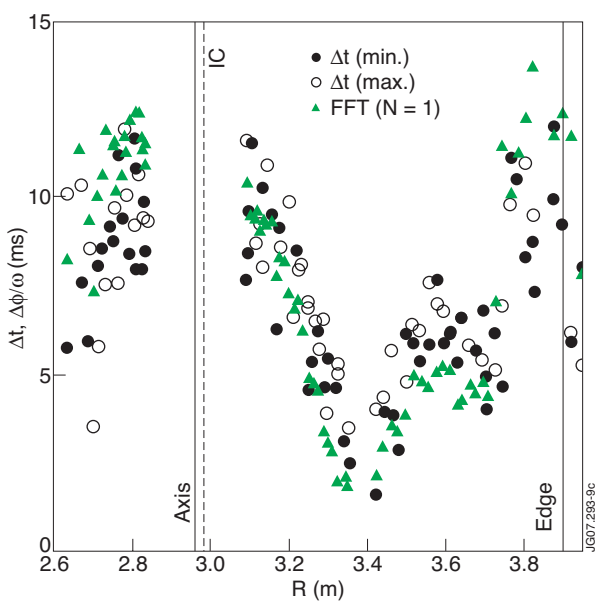

Figure 6: Time delays between the electron temperature response of the various ECE channels and the RF power modulation compared with the normalised phases (Δϕ/ω) obtained in the FFT (N=1) analysis (▲) for the MH regime shown in Fig.5b. An interval of 0.2s was used for the FFT and the represented BIS time delays are the averaged values of the single time delays at the minima (●) and maxima (○) of the ECE signals.*

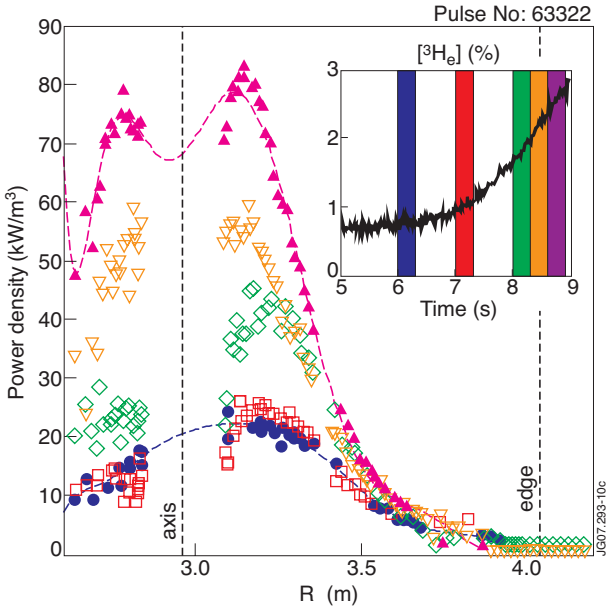

Figure 7: Evolution of the electron RF absorption profile estimated with the BIS procedure when the 3He minority concentration is increased from ~0.8% to ~3%, evidencing the transition from the minority heating regime to the mode-conversion regime in an inverted (3He)H ICRH experiment in JET (#63322).*

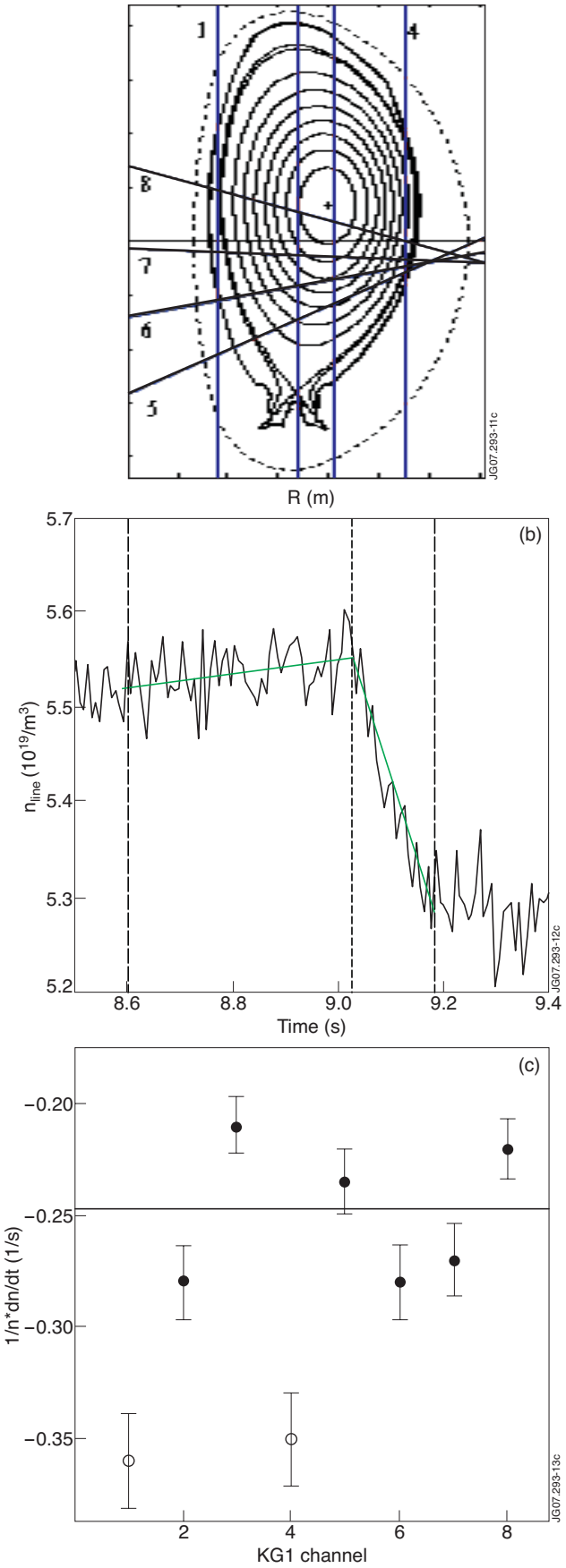

Figure 8: (a) Lines-of-sight of the fast interferometer diagnostic (KG1) in JET; (b) Example of one KG1 signal (channel 3) illustrating the evaluation of the change in the slope due to the external power change; (c) Values of the normalized slopes $1/n_\alpha(dn_\alpha/dt)$ *of the KG1 signals after the power break and the averaged value used for the BIS analysis (dashed line).*

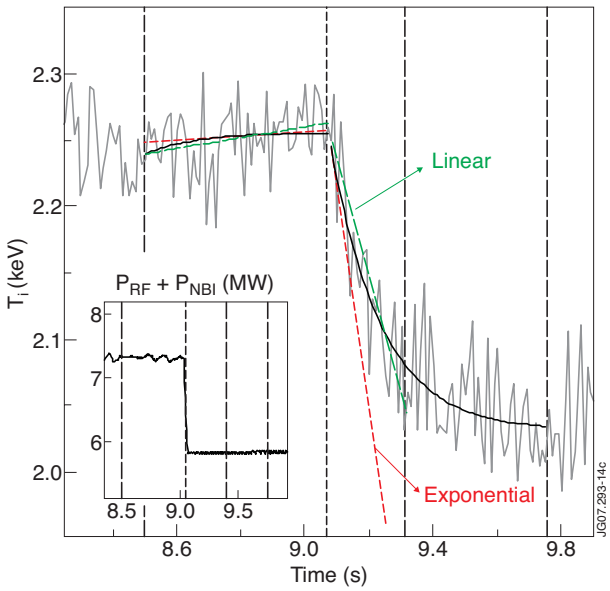

Figure 9: Examples of charge-exchange (KS5) ion temperature measurements at R=*3.42m during an RF power step illustrating the exponential and linear functions fitted to the experimental data to evaluate the dT/dt slopes close to the power break (dashed and dotted lines).*

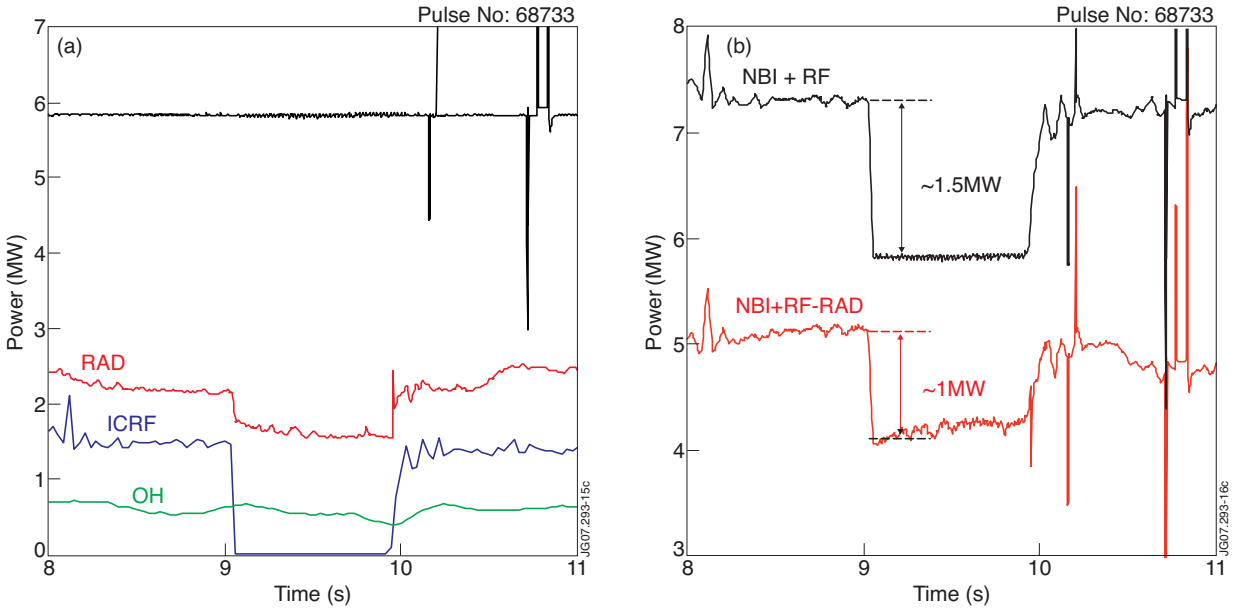

Figure 10: (a) Time traces of neutral-beam (NBI), ion-cyclotron (ICRF), ohmic (OH) and radiated (RAD) power levels in Pulse No: 68733 at JET; (b) Effective power change during the ICRF switch-off (t=9s) when either including or omitting the variation of the radiation losses.

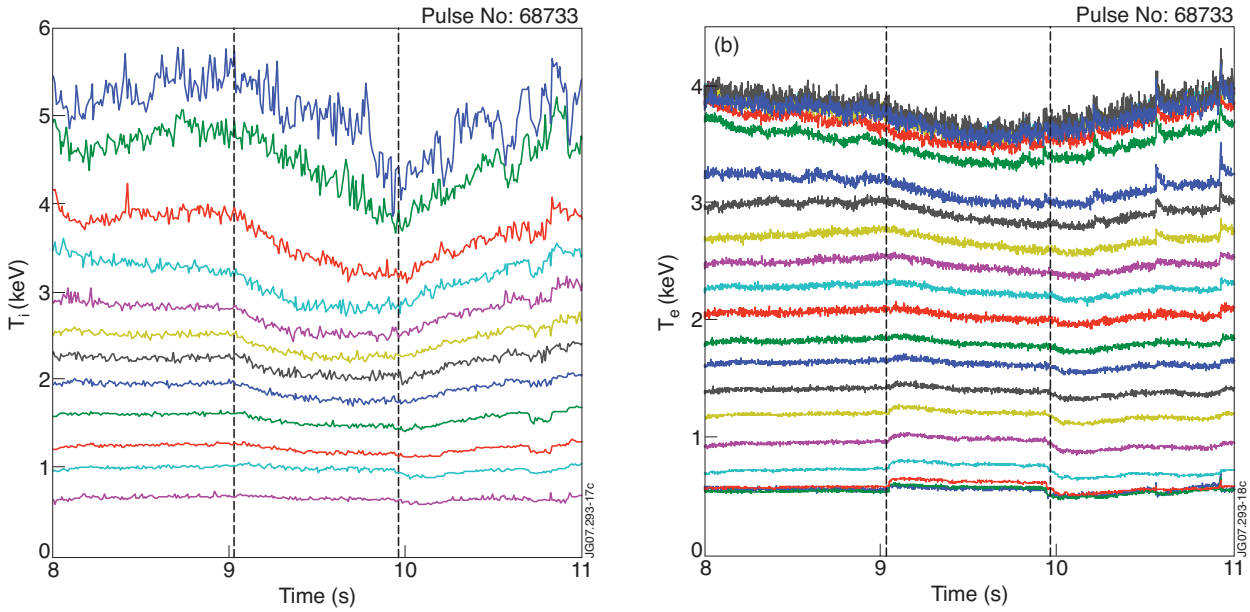

Figure 11: (a) Ion temperature (KS5) and (b) electron temperature (KK3) measured during a mICRF power switch-off (Fig.10) in a Deuterium majority ICRH experiment at JET (Pulse No:68733).

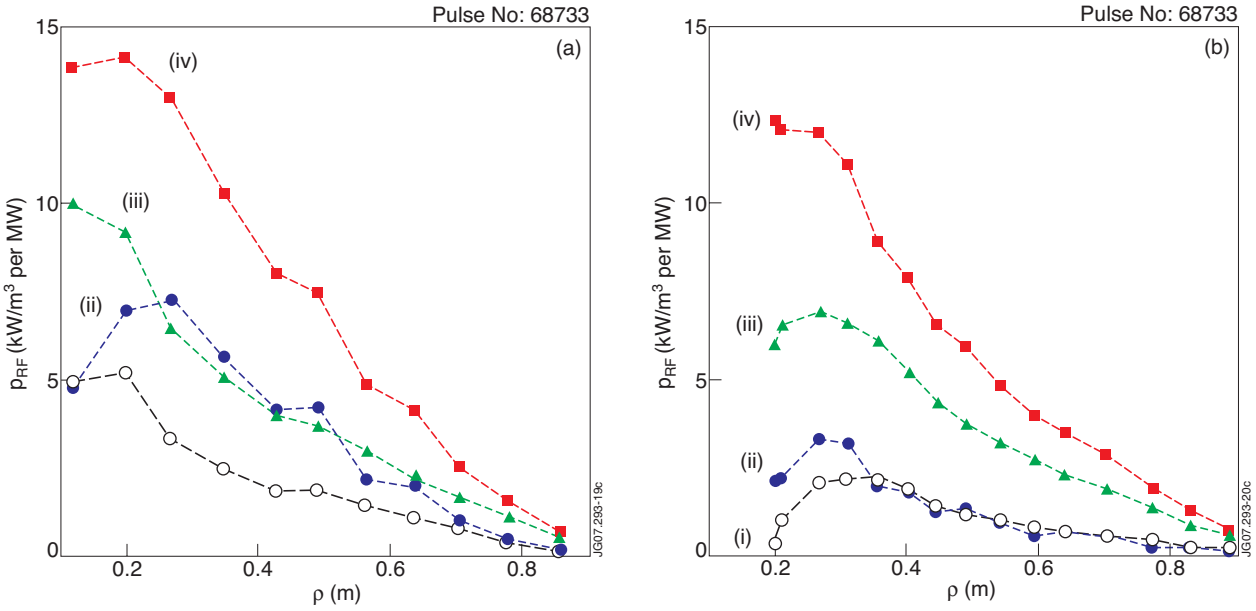

Figure 12: Power absorption profiles (per MW of applied power) obtained with the improved BIS analysis to the RF power step for the ions (a) and for the electrons (b) using 4 different minimization procedures: (i) linear T_α fit + constant n_0; (ii) exponential T_α fit + constant n_0; (iii) linear T_α and n_α fits; (iv) exponential T_α and n_α fits

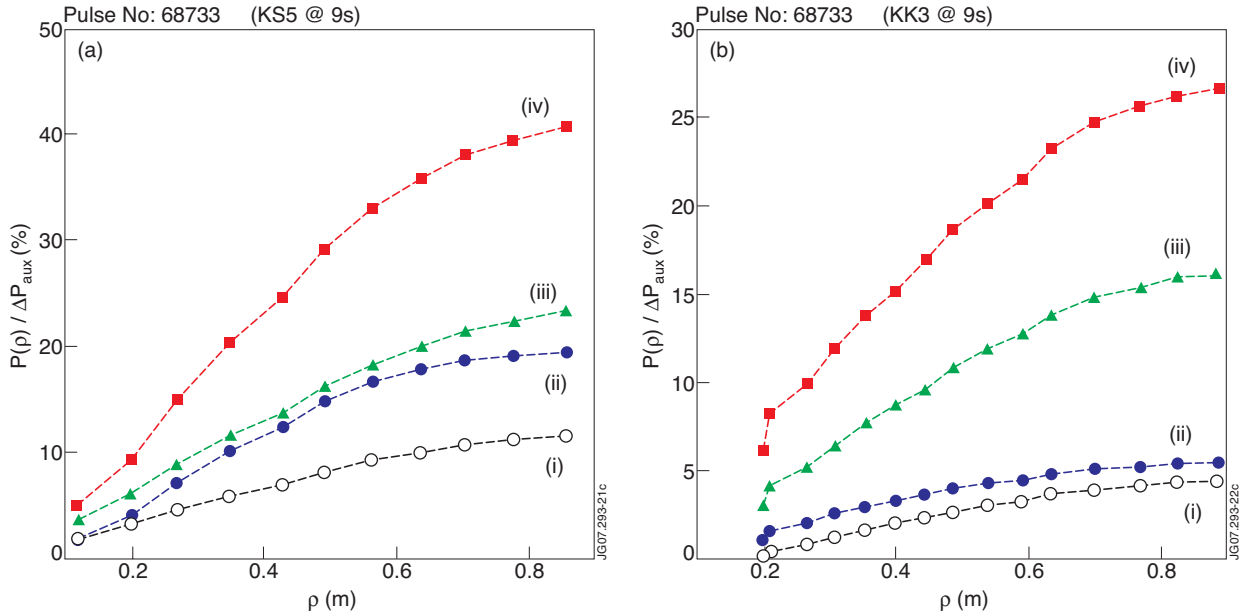

Figure 13: Integrated power values normalized to the nominal ICRF power step (1.5MW) obtained for the ions (a) and for the electrons (b) with the improved BIS analysis using the 4 fitting combinations described in Fig.12.

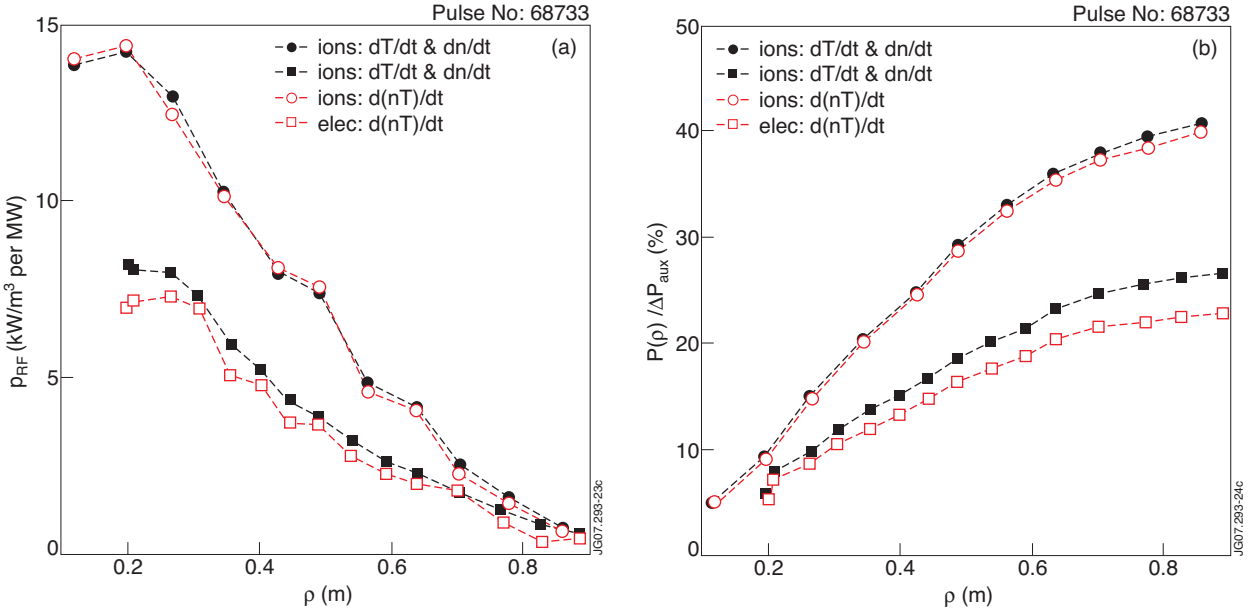

Figure 14: (a) Power absorption profiles and (b) integrated power levels obtained for the ions and for the electrons in Pulse No: 68733 with two different methods: (i) independent evaluation of the dT_α/dt and dn_α/dt slopes (full symbols); (ii) evaluation of the slopes of the reconstructed energy density signal $d(n_\alpha T_\alpha)/dt$ (hollow symbols). In both cases an exponential fit was used for computing the slopes near the power step.

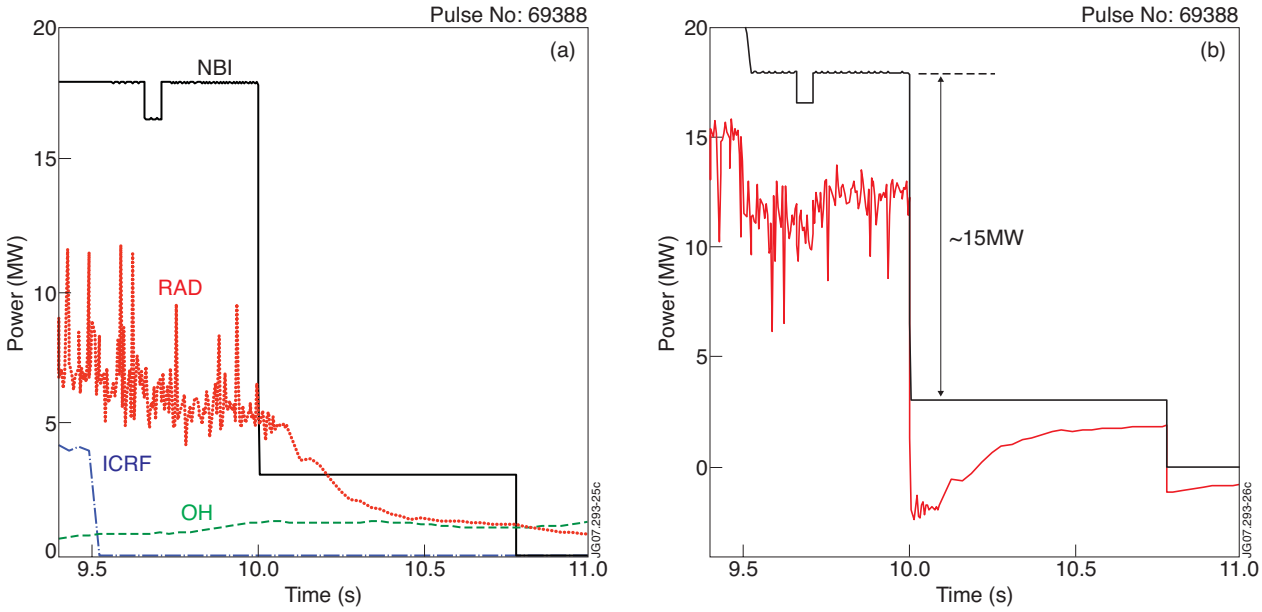

Figure 15: (a) Time traces of neutral-beam (NBI), ion-cyclotron (ICRF), ohmic (OH) and radiated (RAD) power levels in Pulse No: 69388 at JET; (b) Effective power change during the NBI switch-off (t=10s) when including or omitting the variation of the radiation losses.

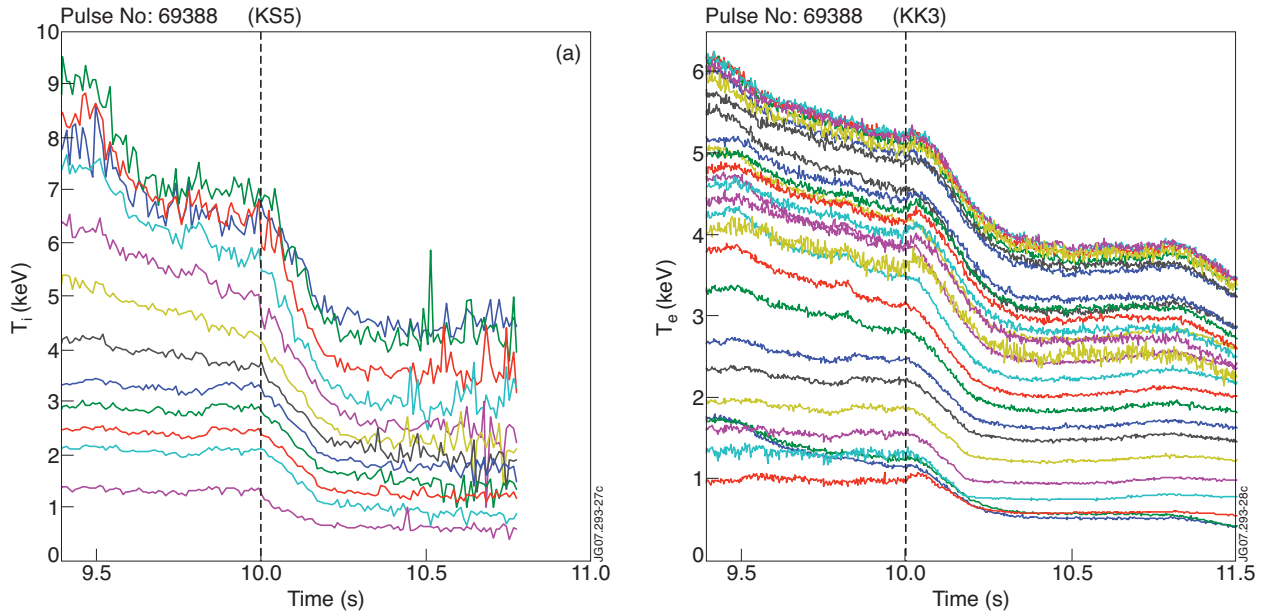

Figure 16: (a) Ion temperature (KS5) and (b) electron temperature (KK3) measured during the switch-off of the NBI power (Fig.15) in a (^{3}He)D plasma at JET (Pulse No:69388). The ICRF was shutdown at t=9.5s.

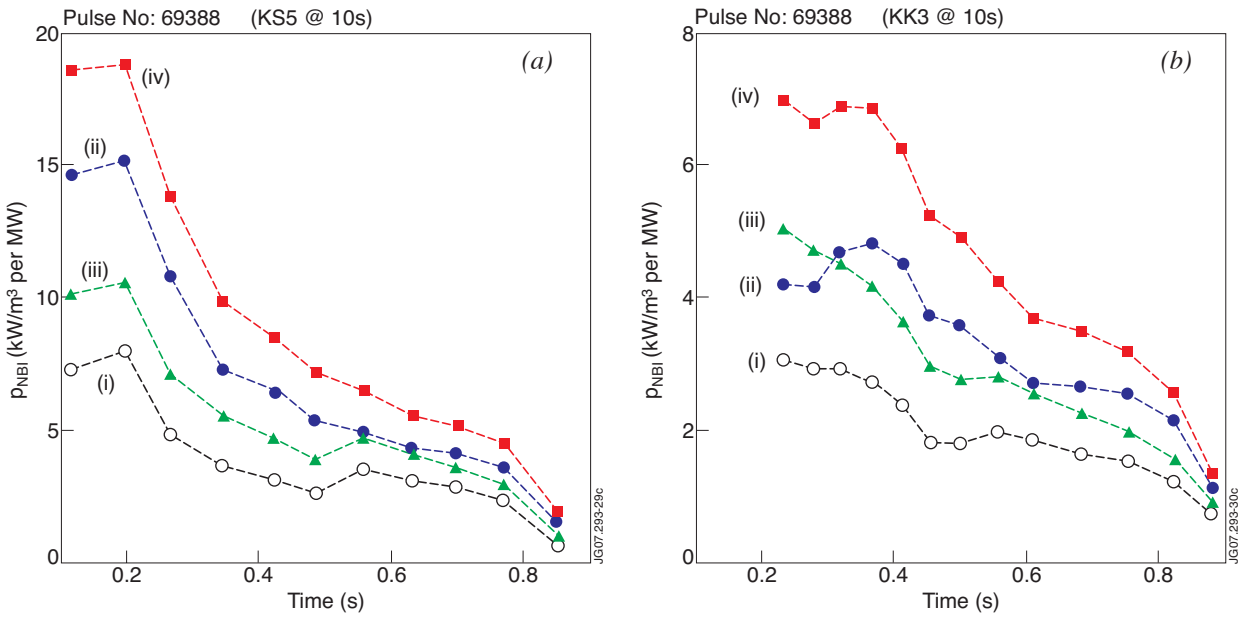

Figure 17: Power absorption profiles (per MW of launched power) obtained with the improved BIS analysis applied to the NBI power step for the ions (a) and for the electrons (b) using 4 different minimization procedures: (i) linear T_α fit + constant n_0; (ii) exponential T_α fit + constant n_0; (iii) linear T_α and n_α fits; (iv) exponential T_α and n_α fits.

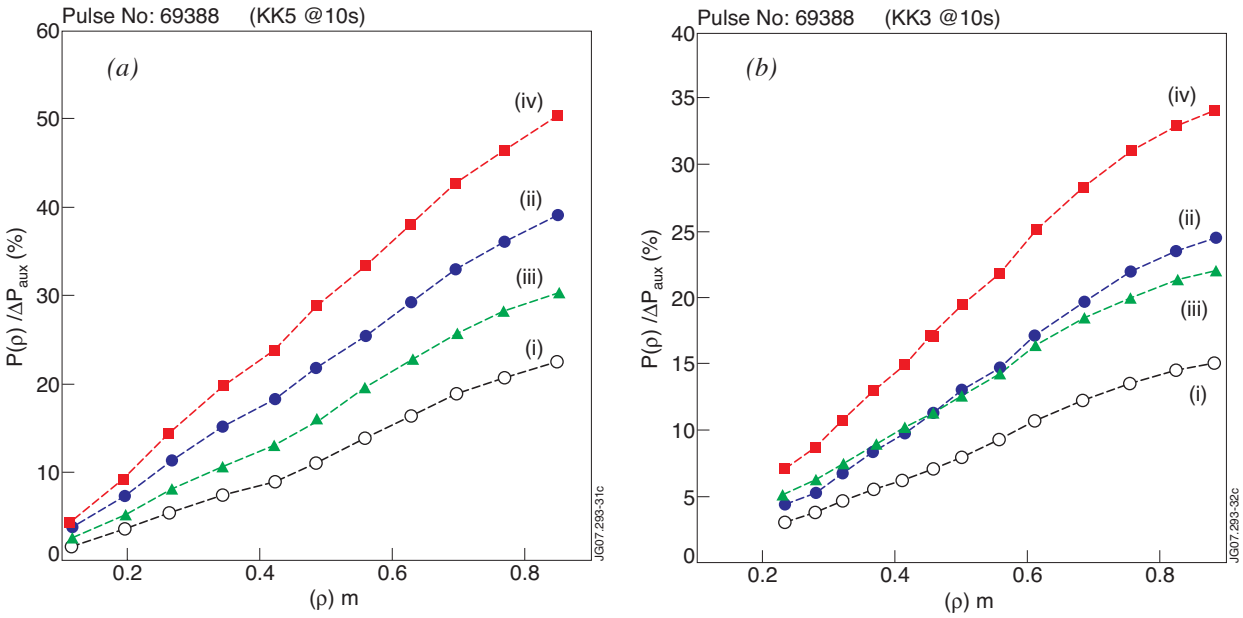

Figure 18: Integrated power values normalized to the NBI power step (15MW) obtained for the ions (a) and for the electrons (b) with the improved BIS analysis using the 4 fitting combinations described in Fig.17.